Rock and Soil Mechanics

Volume 41 | Issue 2 Article 1

9-27-2020

Study on creep characteristics of claystone under thermo-hydro-mechanical coupling

Wei-zhong CHEN
State Key Laboratory of Geomechanics and Geotechnical Engineering, Institute of Rock and Soil Mechanics, Chinese Academy of Sciences, Wuhan, Hubei 430071, China

Fan-fan LI
University of Chinese Academy of Sciences, Beijing 100049, China

Jiang LEI
University of Chinese Academy of Sciences, Beijing 100049, China

Hong-dan YU
State Key Laboratory of Geomechanics and Geotechnical Engineering, Institute of Rock and Soil Mechanics, Chinese Academy of Sciences, Wuhan, Hubei 430071, China

See next page for additional authors

Custom Citation

CHEN Wei-zhong, LI Fan-fan, LEI Jiang, YU Hong-dan, MA Yong-shang, . Study on creep characteristics of claystone under thermo-hydro- mechanical coupling[J]. Rock and Soil Mechanics, 2020, 41(2): 379-388.

Study on creep characteristics of claystone under thermo-hydro- mechanical coupling

Authors

Wei-zhong CHEN, Fan-fan LI, Jiang LEI, Hong-dan YU, and Yong-shang MA

Rock and Soil Mechanics 2020 41(2): 379–388 ISSN 1000–7598
https: //doi.org/10.16285/j.rsm.2019.5016 rocksoilmech.researchcommons.org/journal

Study on creep characteristics of claystone under thermo-hydro-mechanical coupling

CHEN Wei-zhong[1], LI Fan-fan[1, 2], LEI Jiang[1, 2], YU Hong-dan[1], MA Yong-shang[1, 2]

1. State Key Laboratory of Geomechanics and Geotechnical Engineering, Institute of Rock and Soil Mechanics, Chinese Academy of Sciences, Wuhan, Hubei 430071, China

2. University of Chinese Academy of Sciences, Beijing 100049, China

Abstract: As an alternative medium for the underground disposal of radioactive waste, claystone will be in the complex conditions of thermo-hydro-mechanical coupling for a long time. In order to study the long-term stability of surrounding rocks, a series of heating-cooling drainage creep tests on claystone was carried out under different confining pressures and deviatoric stresses, and the following conclusions were drawn. The rise of temperature will increase the creep rate of claystone, and extend the time of decay creep stage. But during the cooling process, the samples mainly experience shrinkage deformation without obvious creep deformation being observed. The decrease of confining pressure and the increase of deviatoric stress will increase the creep rate of claystone, and this effect will be significantly aggravated with the increase of temperature. Based on the experimental results, creep hardening, creep damage and thermal damage were introduced on the basis of Perzyna overstress theory, and a coupled thermo-hydro-mechanical creep model for claystone was established. The model was numerically implemented in ABAQUS and its subroutines. The comparison between the simulation results and test results demonstrates that the model can effectively describe the creep characteristics of claystone under thermo-hydro-mechanical coupling.

Keywords: claystone; temperature; creep; damage; overstress

1 Introduction

At present, the treatment of nuclear waste in the world mainly uses the method of deep geological disposal. In the deep underground environment, due to the heat release of the nuclear waste itself and the existence of groundwater, the surrounding rock of the repository will be under the condition of thermo-hydro-mechanical coupling for a long time. Claystone is one of the commonly used alternative media for nuclear waste disposal (such as Opalinus clay in Switzerland, Callovo-Oxfordian clay in France, and Boom clay in Belgium). In order to ensure the long-term safety of nuclear waste repositories, in-depth study of creep characteristics of claystone under the condition of thermo-hydro-mechanical coupling is particularly important.

Regarding the existing research on the creep characteristics of claystone under thermo-hydro-mechanical coupling conditions, Li et al.[1] performed heating and cooling tests with a range of 5–25℃ on the original and remodelled samples of sensitive claystone. The remodelled samples are much less sensitive to temperature during the creep process in comparison with the original samples, and it is believed that this is because the adhesion between the particles of the remodelled samples is destroyed, resulting in a decrease in its sensitivity to temperature. Kurz et al.[2] analysed the heating creep tests of normally consolidated and lightly overconsolidated claystone, and attributed the viscoplastic deformation of the samples to plastic deformation, and introduced the creep rate coefficient affected by temperature and plastic deformation to describe the viscoplastic deformation. A semi-empirical thermal visco-elasto-plastic model is established. Cui et al.[3] systematically studied the time dependence of thermal deformation of claystone. The results show that the thermal deformation rate gradually decreases with time, the higher the temperature, the faster the thermal deformation rate, and the relationship between the thermal creep rate and temperature can be described using an exponential function. Belmokhtar et al.[4] performed a heating test on the drained Callovo-Oxfordian Claystone under isotropic pressure consolidation conditions, which found that the volumetric creep strain of claystone under heating conditions was significantly increased, and the test curve was simulated using the Kelvin-Voigt model. Campanella et al.[5] performed a series of heating creep tests on illite and San Francisco Bay mud, and discovered that the influence of temperature on the creep effect is related to the temperature-stress loading path. Djeran et al.[6] believed that the creep deformation of claystone can be divided into dissipative deformation of pore water pressure and viscous deformation of

Received: 7 January 2019 Revised: 28 May 2019
This work was supported by the National Natural Science Foundation of China (51979266, 51879258) and the Cooperation Project of the European Underground Research Infrastructure for Disposal of Nuclear Waste in Clay Environment, Mol, Belgium(EUR-12-110).
First author: CHEN Wei-zhong, male, born in 1968, PhD, Professor, Doctoral supervisor, Research interest: tunnel and underground. E-mail: wzchen@whrsm.ac.cn

claystone matrix. By conducting a series of undrained heating creep tests on Boom clay, it was found that the increase in temperature would increase the viscous deformation of the claystone matrix and the reduce the threshold value of the deviatoric creep stress. Burghignoli et al. [7] studied Todi, Fiumicino, and Bologna clays and found that changes in temperature would affect the viscosity coefficient of the claystone matrix, and they believed that this factor must be considered when establishing a creep model for claystone. Gao et al. [8] comprehensively considered the effects of temperature on elastic deformation, viscous flow and structural damage, and introduced thermal expansion coefficients, viscous attenuation coefficients and damage variables on the basis of the Nishihara model to establish a thermal visco-elasto-plastic damage model. Li et al.[9] carried out an experimental research on the creep characteristics of soft rocks under heating, and discussed the creep law of soft rock under heating conditions, indicating that the creep process of soft rock is a dynamic change of "strengthening" and "weakening". In the process of soft rock creep, force is the dominant factor while heat is the auxiliary factor. Shu et al.[10] analysed the effect of stress level and pore water pressure on creep characteristics of soft rocks, and proposed a nonlinear viscosity coefficient Newton element, which was connected in series with the Nishihara model to obtain a nonlinear visco-elasto-plastic creep model for soft rock.

After nearly half a century of development, significant amount of research has been dedicated on studying the creep characteristics of rocks. However, the research on the effect of temperature on the creep characteristics of rocks still needs to be further strengthened, especially on the claystone with obvious creep behaviours.

This paper studies claystone to systematically analyses the influence rules of confining pressure, deviatoric stress, and temperature on the creep characteristics of claystone by conducting a series of heating-cooling drainage creep tests on claystone under different confining pressure and deviatoric stress conditions. The results of the creep test show that the creep rate of claystone is related to temperature, confining pressure, deviatoric stress, and creep strain. The author introduced the concepts of creep hardening, creep damage, and thermal damage based on the Perzyna overstress theory to establish a coupled thermo-hydro-mechanical creep model for claystone. The model was numerically implemented in ABAQUS and its subroutines. The comparison between the results of simulation and test verifies that the proposed model can effectively reflect the creep characteristics of claystone under heating conditions.

2 Test preparation

2.1 Test equipment and sample preparation

The heating-cooling drainage creep test was performed on a parallel-type temperature-seepage-stress coupling triaxial rheometer[11] independently developed for soft rock by the Wuhan Institute of Rock and Soil Mechanics, Chinese Academy of Sciences. The instrument is mainly composed of the axial loading system, confining pressure loading system, hydraulic pressure loading system, temperature control system, and deformation monitoring and recording system. Axial force measurement uses the German HBM sensor with a measurement range of 0–50 kN, measurement accuracy of 0.04%, and a temperature compensation range of –30–85℃; the DRUCK sensor is used for measuring the confining pressure and water pressure with a measurement range of 0–5 MPa, measurement accuracy of 0.1%, and a temperature compensation range of –40–125℃; the measurement accuracy of the temperature controller is 0.5 ℃ with a control range up to 120 ℃; deformation measurement is performed using the LVDT deformation sensor with a measurement range of 0–10 mm and measurement accuracy of 0.1%. The test machine is shown in Fig.1.

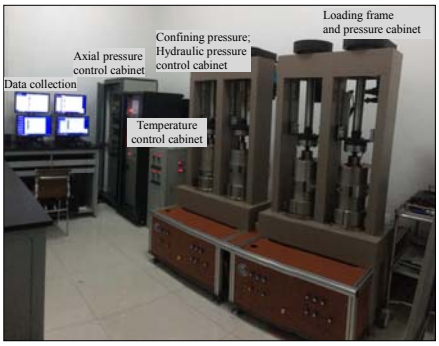

Fig.1 Parallel-type temperature-seepage-stress coupling triaxial rheometer for thermal-hydro-mechanical (THM) coupling in soft rock[11]

The specimens were processed into standard sample size of 38 mm × 76 mm by blade cutting and sandpaper sanding with the preparation procedures shown in Fig.2. The basic information of the claystone sample is shown in Table 1.

2.2 Test procedure

The thermo-mechanical path of the heating-cooling drainage creep test is shown in Fig. 3.

Stage 1 (I–II), i.e. saturation stage: The surrounding rocks at the project site are saturated, however water will be lost during transportation and storage. Therefore, the prepared samples need to be re-saturated in the pressure chamber. This is achieved by firstly applying a certain amount of confining pressure and water pressure to ensure the stability of the testing

machine, and then restore the stress state of sample to the original effective stress state for saturation. Once the expansion and deformation of the sample is stable, measure the Skempton B coefficient of the sample to determine whether the sample is saturated, if saturated, increase the confining pressure and water pressure to values specified in the creep stage. Thereafter, the confining pressure and water pressure remain unchanged until the end of the test.

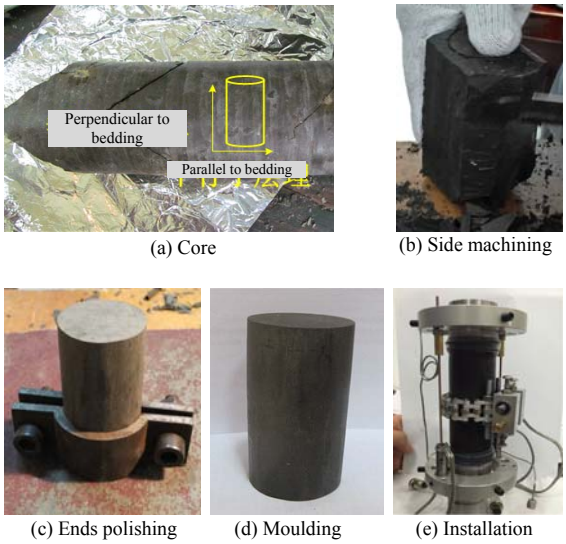

(a) Core (b) Side machining

(c) Ends polishing (d) Moulding (e) Installation

Fig.2 Processing and installation of claystone samples

Table 1 Basic information of claystone samples

Sample label	Density / (g • cm^{-3})	Water content / %	Dry density / (g • cm^{-3})	Void ratio	saturation / %
LTHM-1	2.04	23.96	1.64	0.67	98.28
LTHM-2	2.04	23.96	1.64	0.67	98.28
LTHM-3	2.02	22.42	1.65	0.66	93.32

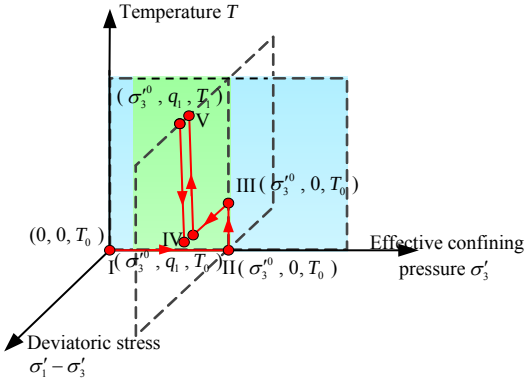

Fig.3 Thermo-mechanical loading path of the heating-cooling drainage creep test

Figure 4 shows the path of confining pressure and water pressure in phase 1 of the sample LTHM-2 (the time on the abscissa in the figure is for reference only). The stress paths of the other two samples are similar(as listed in Table 2).

Stage 2 (II–III): After the deformation in the previous stage is stabilised, heat up the sample to 40 at 0.3℃ / h.

Stage 3 (III–IV): After the deformation in the previous stage is stabilised, apply a deviatoric stress specified by the test at a rate of 0.004 2 MPa / s.

Stage 4 (IV–V): After the deformation of the specimen is stabilised under the effect of the deviatoric stress, the magnitude of the deviatoric stress of the specimen is kept constant, and a heating-cooling cycle is started, and the temperature change rate is 0.3℃ / h.

This test mainly considers the influence of temperature, confining pressure and deviatoric stress on the creep characteristics of claystone.

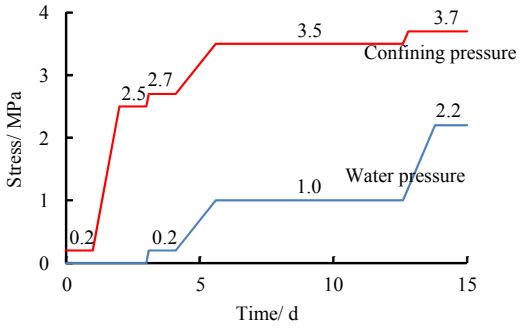

Fig.4 Confining pressure and hydraulic pressure loading path during stage 1 for sample LTHM-2

Table 2 Test conditions of creep stage

Sample label	Condfining pressure / MPa	Water pressure / MPa	Deviatoric stress / MPa	Temperature /℃
LTHM-1	4.7	2.2	1.5	40→60→80→60→40
LTHM-2	3.7	2.2	1.5	40→60→80→60→40
LTHM-3	3.7	2.2	0.5	40→60→80→60→40

3 Test results and analysis

The average test period for each sample is 4 000 h, of which the saturation stage is 500 h and the drainage creep stage is 3 500 h. The focus of this article is the creep law of claystone. Therefore, only one of the typical test results is used to describe the deformation law of the sample in the saturation stage.

The strain curve of the sample LTHM-3 in the saturation stage is shown in Fig. 5. It can be clearly seen from the figure that when the isotropic pressure was applied, the specimen was obviously compressed in both the axial and radial directions. When the water pressure was added, the specimen had obvious expansion and deformation in both the axial and radial directions, which was caused by the water absorption and expansion of clay minerals inside the claystone [12]. When the confining pressure of 3.5 MPa and water pressure of 1.0 MPa

were changed to 3.7 MPa and 2.2 MPa, respectively, the specimen experienced significant expansion deformation again in the axial and radial directions due to reduction of effective stress.

Figure 6 shows that the axial creep strain curve of each sample during the heating-cooling phase. The sample LTHM-3 was not completed due to the heating system failure.

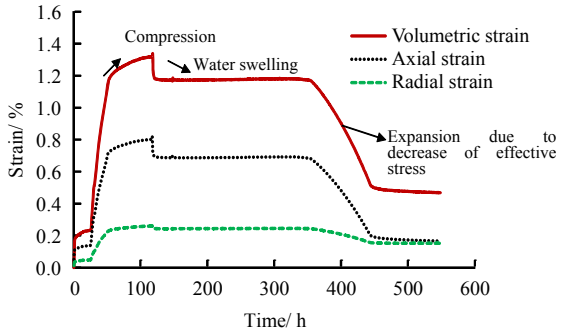

Fig.5 Strain curves during saturation stage for LTHM-3

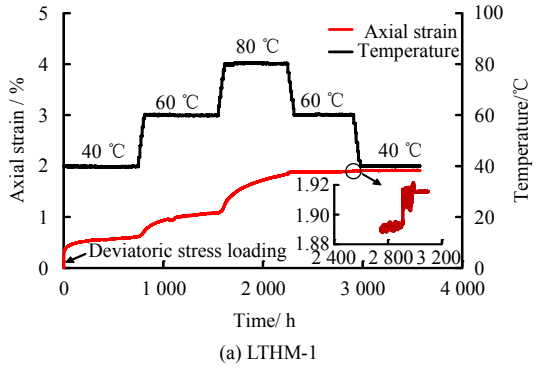

(a) LTHM-1

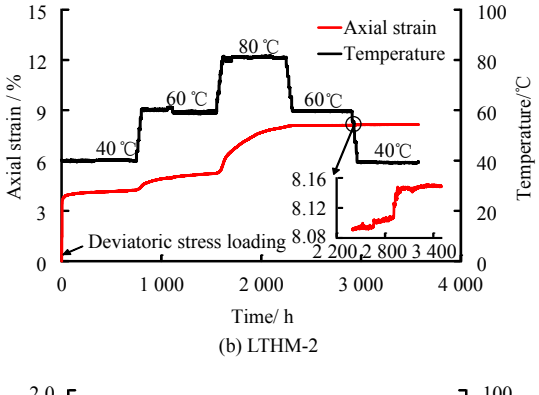

(b) LTHM-2

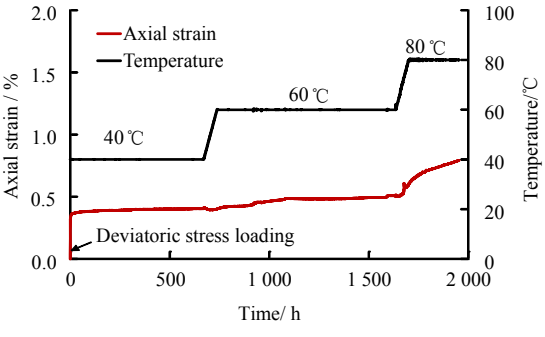

(c) LTHM-3

Fig.6 Axial strain curves of samples during creep stage

Figure 7 transforms the creep curve during the heating phase into the form of axial creep rate versus time. Since the creep is not obvious during the cooling stage, it is not included in the figure.

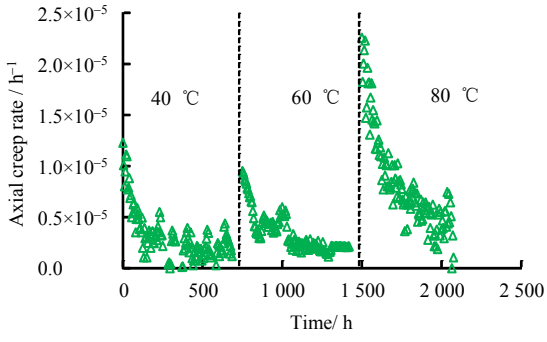

(a) LTHM-1

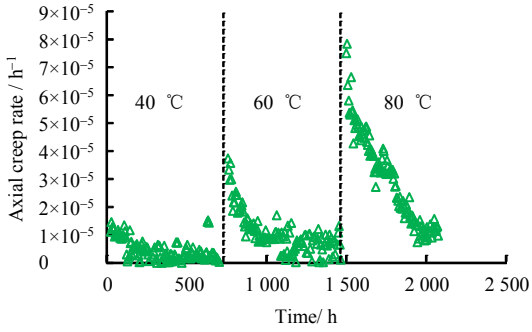

(b) LTHM-2

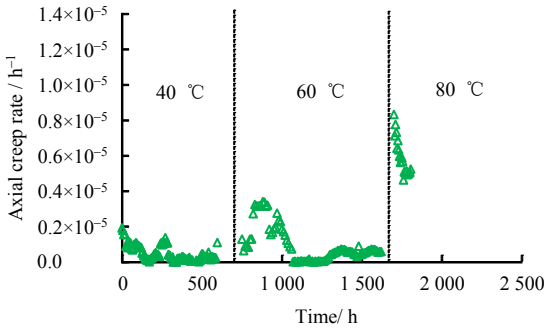

(c) LTHM-3

Fig.7 Axial creep rate during creep stage

It can be seen from Figs. 6 and 7 that during the heating process, the claystone experiences obvious creep deformation, but during the cooling process, there is only a small amount of cold shrinkage deformation and no obvious creep deformation. Moreover, the creep deformation of the samples during the heating stage is obviously aggravated with the increase of temperature.

In order to further explore the effects of temperature, deviatoric stress and confining pressure on the creep characteristics of claystone, the respective strain, time of decay creep stage, initial creep change rate and steady creep change

rate of the three samples after 600 h of creep at each stage during the heating process are extracted and reported in Tables 3–6.

It can be seen from Table 3 that the creep deformation of claystone will increase significantly with the increase of temperature, and decrease significantly with the increase of confining pressure. The increase of deviatoric stress will obviously increase the creep deformation of claystone.

It can be seen from Table 4 that the increase of temperature will result in a longer transition for claystone to enter the steady-state creep stage from the decay creep stage.

Table 3 Creep strain after 600 h in each stage during heating process

Sample label	Test conditions		Creep strain at different temperatures / %		
	Confining pressure / MPa	Deviatoric stress / MPa	40 ℃	60 ℃	80 ℃
LTHM-1	4.7	1.5	0.18	0.29	0.51
LTHM-2	3.7	1.5	0.38	0.70	2.04
LTHM-3	3.7	0.5	0.03	0.07	—

Table 4 Time of decay creep at each stage during heating process

Sample label	Test conditions		decay creep stage duration/ h		
	Confining pressure / MPa	Deviatoric stress / MPa	40 ℃	60 ℃	80 ℃
LTHM-1	4.7	1.5	200	300	450
LTHM-2	3.7	1.5	150	200	500
LTHM-3	3.7	0.5	170	300	—

Table 5 Initial creep rate at each stage during heating process

Sample label	Test conditions		Initial creep rate / h^{-1}		
	Confining pressure / MPa	Deviatoric stress / MPa	40 ℃	60 ℃	80 ℃
LTHM-1	4.7	1.5	1.2×10^{-5}	1.5×10^{-5}	2.1×10^{-5}
LTHM-2	3.7	1.5	1.4×10^{-5}	3.7×10^{-5}	7.8×10^{-5}
LTHM-3	3.7	0.5	2.0×10^{-6}	1.6×10^{-6}	8.3×10^{-6}

Table 6 Steady-creep rate at each stage during heating process

Sample label	Test conditions		Steady-creep rate / h^{-1}		
	Confining pressure / MPa	Deviatoric stress / MPa	40 ℃	60 ℃	80 ℃
LTHM-1	4.7	1.5	1.6×10^{-6}	2.3×10^{-6}	4.5×10^{-6}
LTHM-2	3.7	1.5	1.7×10^{-6}	3.2×10^{-6}	12.0×10^{-6}
LTHM-3	3.7	0.5	3.2×10^{-7}	5.6×10^{-7}	—

It can be seen from Table 5 that an increase in temperature will significantly increase the initial creep rate of claystone; an increase in confining pressure will significantly reduce the initial creep rate of claystone; the greater the deviatoric stress, the greater the initial creep rate of claystone.

It can be seen from Table 6 that as the temperature increases, the axial creep rate of claystone during the steady-state creep phase increases significantly; the higher the confining pressure, the smaller the increase of the axial creep rates of claystone during the steady-state creep phase; the increase of the deviatoric stress will obviously increase the steady-state creep rate of claystone.

In summary, the following conclusions can be drawn:

(1) The creep of the claystone during heating mainly includes two stages: the decay creep stage and the steady state creep stage (there is no obvious accelerated creep stage in this test process). However, during the process of temperature decreases, the claystone has experienced a small amount of cold shrinkage deformation, but there is no obvious creep deformation. This is because that the increase in temperature will reduce the viscosity and long-term strength of the claystone[13]. Under the original stress, the state of the sample cannot be maintained. The sample will first produce a deformation similar to loading. After stabilisation, as the creep strain increases, the specimen will undergo the decay creep stage and steady state creep stage. During the cooling process, the creep phenomenon will become insignificant because the viscosity of the sample will gradually recover.

(2) The increase of temperature and the increase of partial stress will increase the creep deformation and creep rate of claystone, but the increase of confining pressure will reduce the creep deformation and creep rate.

(3) The influence of confining pressure on the creep properties of claystone is affected by temperature. Comparing the results of the samples LTHM-1 and LTHM-2, it can be seen that during heating, the difference in the creep deformation and creep rate of the claystone under different confining pressures becomes more obvious as the temperature increases.

(4) The influence of deviatoric stress on the creep characteristics of claystone is also affected by temperature. Comparing the results of samples LTHM-2 and LTHM-3, it can be seen that during heating, the higher the temperature, the more obvious the difference of creep deformation and creep rate in axial direction caused by the change in deviatoric stress.

4 Coupled thermo-hydro-mechanical creep model

The overstress theory [14–15] assumes that there is a creep yield surface during rock creep, but the stress during creep is not always above the creep yield surface. When the stress is less than or on the creep yield surface, the rock will not creep; when

the stress exceeds the creep yield surface, the specimen begins to creep. The stress beyond the creep yield surface is called overstress. During the creep process, the creep yield surface will harden / soften as the creep strain increases, thus simulating the various stages of creep. The Perzyna overstress theoretical model has the advantages of simple numerical implementation and can describe the long-term mechanical behaviour of materials under complex stress conditions. Many scholars have established viscoplastic models based on this widely recognised model [16–19].

It is assumed that there exists a creep yield surface of claystone. The size of the initial creep yield surface is related to stress and temperature. When the temperature increases, the creep yield surface shrinks under the effects of temperature, the overstress increases, and the creep rate increases significantly. In the decay creep phase, the increase of creep strain will exert a "hardening effect", which will gradually expand the creep yield surface, reduce the overstress, and gradually reduce the creep rate. In the steady-state creep phase, as the creep strain continues to increase, the "hardening effect" tends to be stabilised, the creep yield surface remains unchanged, and the creep rate of the rock mass remains stable. When the creep strain continues to increase and the micro-cracks inside the rock mass develop significantly, the damage caused by creep will cause the shrinkage of the creep yield surface and the increase of overstress, the gradual increase of creep rate, and eventually the rock mass will fail, this process is regarded as the accelerated creep phase. This paper introduces the equations of creep hardening, creep damage and thermal damage based on Perzyna's overstress theory in order to establish a reasonable model to describe the creep characteristics of claystone.

4.1 Creep yield surface and creep flow law

As shown in Fig.8, this paper considers the two types of creep in claystone under different stress states: shear creep and consolidation creep. When the stress state exceeds the shear creep yield surface, shear creep occurs. Similarly, when the stress state exceeds the consolidation creep yield surface, consolidation creep occurs.

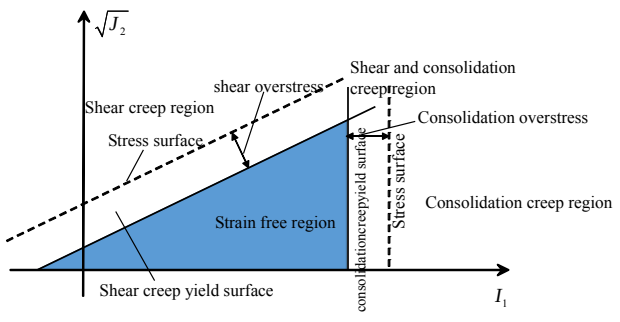

Fig.8 Creep yield surface and creep region

The function expressions of the shear creep yield surface F_c^s and the consolidated creep yield surface F_c^c are as follows:

$$\left.\begin{aligned} F_c^s &= \sqrt{3J_2} - \alpha_c I_1 - k_c = 0 \\ F_c^c &= I_1 - \overline{p}_h = 0 \end{aligned}\right\} \tag{1}$$

where I_1 is the first invariant of stress; J_2 is the second invariant of deviatoric stress; α_c、k_c and $\overline{p}_h$ are the model parameters related to creep hardening, creep damage, and thermal damage, respectively (the calculation formulae are described later).

Assuming the creep meets the flow rule, the shear creep potential function G_c^s and the consolidation creep potential function G_c^c are

$$\left.\begin{aligned} G_c^s &= \sqrt{\left[\frac{0.1k_0}{(1-\alpha_0/3)}\alpha_0\right]^2 + 3J_2} - \alpha_0 I_1 \\ G_c^c &= \sqrt{\left(I_1 - \overline{p}_{h0}\right)^2 + \left(R\sqrt{3J_2}\right)^2} \end{aligned}\right\} \tag{2}$$

where α_0, k_0 and $\overline{p}_{h0}$ are the model parameters, respectively.

According to the flow rule, the shear creep rate tensor $\dot{\boldsymbol{\varepsilon}}_c^s$ and the consolidation creep rate tensor $\dot{\boldsymbol{\varepsilon}}_c^c$ are calculated as

$$\left.\begin{aligned} \dot{\boldsymbol{\varepsilon}}_c^s &= \frac{1}{\mu_s}\left\langle\frac{f_c^s}{f_0}\right\rangle^n \frac{\partial G_c^s}{\partial \boldsymbol{\sigma}} \\ \dot{\boldsymbol{\varepsilon}}_c^c &= \frac{1}{\mu_c}\left\langle\frac{f_c^c}{f_0}\right\rangle^n \frac{\partial G_c^c}{\partial \boldsymbol{\sigma}} \end{aligned}\right\} \tag{3}$$

where f_c^s is the shear overstress; f_c^c is the consolidation overstress; $f_0 = 1$ MPa is the dimensionless parameter; μ_s and n are model parameters.

The creep rate tensors in different stress states are as following:

$$\dot{\boldsymbol{\varepsilon}}_c = \begin{cases} 0, & \text{Strain free region} \\ \dfrac{1}{\mu_c}\left\langle\dfrac{I_1 - \overline{p}_h}{f_0}\right\rangle^n \dfrac{\partial G_c^c}{\partial \boldsymbol{\sigma}}, & \text{Consolidation creep region} \\ \dfrac{1}{\mu_s}\left\langle\dfrac{\sqrt{3J_2} - \alpha_c I_1 - k_c}{f_0}\right\rangle^n \dfrac{\partial G_c^s}{\partial \boldsymbol{\sigma}}, & \text{Shear creep region} \\ \dfrac{1}{\mu_c}\left\langle\dfrac{I_1 - \overline{p}_h}{f_0}\right\rangle^n \dfrac{\partial G_c^c}{\partial \boldsymbol{\sigma}} + \dfrac{1}{\mu_s}\left\langle\dfrac{\sqrt{3J_2} - \alpha_c I_1 - k_c}{f_0}\right\rangle^n \dfrac{\partial G_c^s}{\partial \boldsymbol{\sigma}}, & \\ \quad \text{Consolidation + shear creep region} & \end{cases} \tag{4}$$

4.2 Creep hardening, creep damage and thermal damage equations

The model believes that in addition to thermal damage, it also affects the hardening of claystone, the creep hardening variable h_{cT} is expressed as

$$h_{cT} = h_{c0} + \frac{b_c\left(1-h_{c0}\right)\left(\xi_c - b_{cT}\Delta T\right)}{\left(1-h_{c0}\right) + b_c\left(\xi_c - b_{cT}\Delta T\right)} \tag{5}$$

where h_{c0}, b_c and b_{cT} the model parameters; ΔT is the

temperature increment; ξ_c is the equivalent creep deviatoric strain, and its expressions are

$$\left.\begin{aligned}\dot{\xi}_c &= \sqrt{\frac{2}{3}\dot{\boldsymbol{e}}_c : \dot{\boldsymbol{e}}_c}\\ \dot{\boldsymbol{e}}_c &= \dot{\boldsymbol{\varepsilon}}_c - \frac{1}{3}\mathrm{tr}\left(\dot{\boldsymbol{\varepsilon}}_c\right)\boldsymbol{\delta}\\ \xi_c &= \xi_c\big|_0 + \int_0^t \dot{\xi}_c \mathrm{d}t\end{aligned}\right\} \tag{6}$$

where $\boldsymbol{\delta}$ is the Kronecker symbol.

Creep damage D_c is expressed as

$$\left.\begin{aligned}\dot{D}_c &= H\left(\xi_c - \xi_c^{\mathrm{th}}\right) c_1 \left[1 - D_c\right]^{c_2} \dot{\xi}_c\\ D_c &= \int_0^t \dot{D}_c \mathrm{d}t\end{aligned}\right\} \tag{7}$$

where ξ_c^{th} is the creep damage threshold; c_1 and c_2 are the model parameters, respectively; $H\left(\xi_c - \xi_c^{\mathrm{th}}\right)$ is the Heaviside function with the expression of

$$H\left(\xi_c - \xi_c^{\mathrm{th}}\right) = \begin{cases}1, & \xi_c \geqslant \xi_c^{\mathrm{th}}\\ 0, & \xi_c < \xi_c^{\mathrm{th}}\end{cases} \tag{8}$$

Considering that heating will cause internal damage to claystone, thermal damage D_{cT} will be introduced with the expression of

$$\left.\begin{aligned}D_{cT} &= 1 - \exp\left[-\beta_{cT}\left(T - T_0\right)\right]\\ T &= \begin{cases}T, & T > T_c\\ T_c, & T \leqslant T_c\end{cases}\end{aligned}\right\} \tag{9}$$

where T_0 is the initial temperature; T_c is the historical maximum temperature; β_{cT} is the model parameter.

Considering the effects of "hardening" and "softening" on creep process, the creep hardening, creep damage and thermal damage are introduced into the creep yield surface. The expression is

$$\left.\begin{aligned}\alpha_c &= \alpha_0\left(1 - D_c\right)\left(1 - D_{cT}\right)h_{cT}\\ k_c &= k_0\left(1 - D_c\right)\left(1 - D_{cT}\right)h_{cT}\\ \overline{p}_h &= \overline{p}_{h0}\exp\left(c_{ch}\varepsilon_c^v\right)\left(1 - D_{cT}\right)\end{aligned}\right\} \tag{10}$$

where ε_c^v is the creep volumetric strain; c_{ch} is the model parameter.

5 Model numerical implementation in ABAQUS

ABAQUS provides users with a series of subroutines. The USDFLD field variable subroutine can update the field variables to achieve the evolution of creep hardening, creep damage and thermal damage throughout the creep process. The CREEP subroutine can define the creep model of plastic materials. The USDFLD subroutine and the CREEP subroutine are jointly used to numerically realise the thermo-hydro-mechanical coupling creep model of claystone in ABAQUS. The flowchart of the subroutines is shown in Fig.9, which is mainly divided into the following steps:

(1) At the beginning of a new incremental step, ABAQUS will give the stress and strain calculated from the previous incremental step, and provide other variables such as the incremental strain, time increment, temperature, etc.

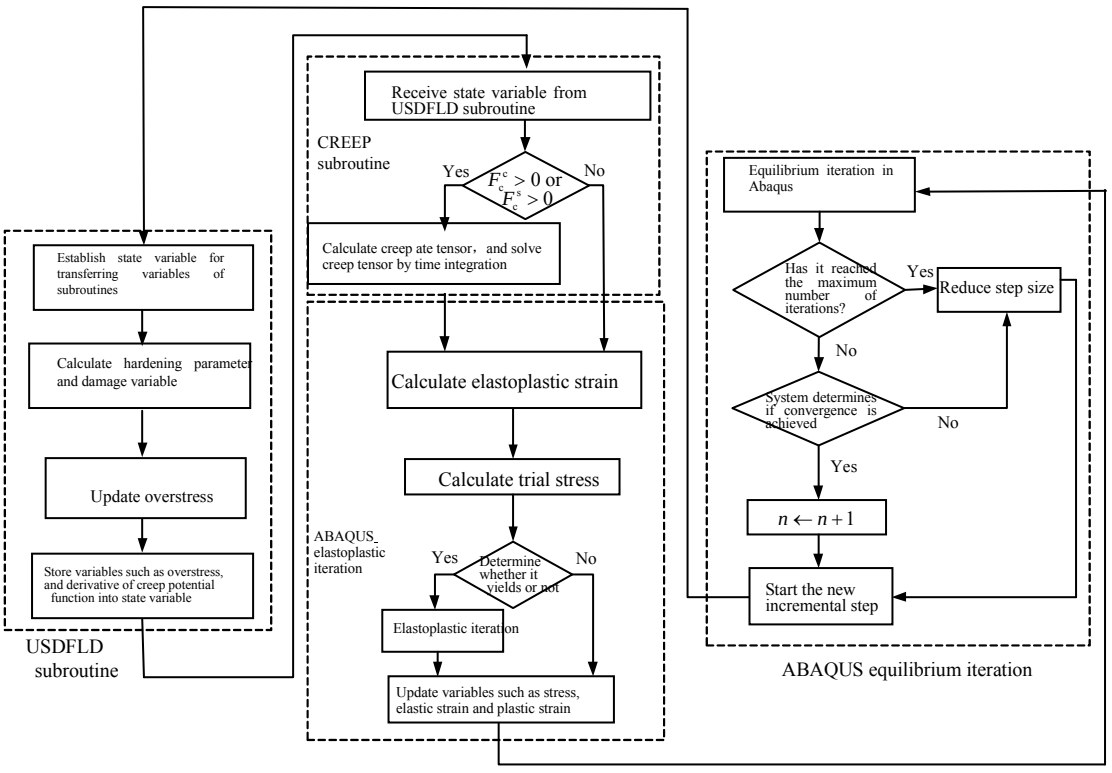

Fig.9 Flow chart of CREEP and USDFLD user subroutines in the ABAQUS code

(2) Calculate the creep hardening parameters, creep damage parameters, and thermal damage parameters through the USDFLD subroutine, and solve the overstress by substituting the solved variables into the creep yield surface. Finally, the solved variables are stored in the state variables.

(3) According to the creep yield surface, determine which case of the Eq. (4) the creep occurs as, and calculate the corresponding creep rate. Integrate the calculated creep rate through the creep subroutine to solve for the creep strain.

(4) The creep strain is subtracted from the given strain increment, and the remaining elastoplastic strain is subjected to plastic equilibrium iteration to solve for the final stress and strain.

(5) Based on the stress and strain calculated above, the finite element model will be used in ABAQUS for equilibrium iteration to determine whether the force and displacement have converged. If converged, proceeds to the next incremental step, if not, reduce the incremental step time and restart the calculation.

The main physical parameters of claystone are the results obtained by other scholars from research on the same claystone [20], as shown in Table 7.

Relevant parameters in the model are obtained by inversion. The comparative test data during the inversion process is the strain curve obtained from the creep test. The inversion uses a joint inversion method integrating Nelder-Mead method and finite element proposed by Jia[21], in which the finite element program is embedded in Nelder-Mead as a separate module and used to solve for the inversion via numerical examples. The objective function expression of inversion is

$$\varphi\left(\beta_{\mathrm{cT}}, b_{\mathrm{cT}}\right)=\sum_{k=1}^{l}\left(\varepsilon_{\mathrm{c}ij}^{\mathrm{calk}}-\varepsilon_{\mathrm{c}ij}^{\mathrm{testk}}\right)^{2} \rightarrow \min \tag{11}$$

where $\varepsilon_{\mathrm{c}ij}^{\mathrm{calk}}$ the creep strain calculated by the finite element calculation; $\varepsilon_{\mathrm{c}ij}^{\mathrm{testk}}$ is the creep strain measured by the test; l is the number of comparison between the test result and the calculation result. during the inversion.

Table 8 shows the model parameter results obtained through the inversion calculation.

Table 7 Basic physical parameters of claystone[20]

Elastic modulus/MPa		Modulus of shear deformation G_{vh0} / MPa	Cohesion / MPa	Preconsolidation pressure/ MPa	Expansion angle/ (°)	Friction angle/ (°)	Permeability coefficient / ($\mathrm{m \cdot s^{-1}}$)		Poisson's ratio	
E_{h0}	E_{v0}						k_{h}	k_{v}	ν_{hh}	ν_{vh}
1 400	700	280	0.4	5	0	18	6×10^{-12}	3×10^{-12}	0.25	0.125

Dry density /($\mathrm{kg \cdot m^{-3}}$)	Void ratio / %	Specific heat capacity/ ($\mathrm{J \cdot kg^{-1} \cdot K^{-1}}$)	Thermal conductivity/ ($\mathrm{W \cdot m^{-1} \cdot K^{-1}}$)		Coefficient of thermal expansion/ $\mathrm{K^{-1}}$	Pore water parameters				
			λ_{h}	λ_{v}		Density / ($\mathrm{kg \cdot m^{-3}}$)	Bulk modulus / GPa	Specific heat capacity /($\mathrm{J \cdot kg^{-1} \cdot K^{-1}}$)	Thermal conductivity / ($\mathrm{W \cdot m^{-1} \cdot K^{-1}}$)	Coefficient of thermal expansion / $\mathrm{K^{-1}}$
1 640	70	740	2.33	1.77	1×10^{-5}	999	2.0	4 200	0.63	4.5×10^{-4}

Table 8 Parameters of the coupled THM creep model

$\bar{p}_{\mathrm{h0}}$ / MPa	k_0 / MPa	μ_{c}	h_{c0}	b_{cT}	c_2	α_0	μ_{s}	n	b_{c}	c_1	β_{cT}
4.7	0.28	2×10^{5}	0.2	0.000 153	0.1	0.13	2×10^{4}	5	180	141	0.011

In order to verify the rationality of the model, a finite element model of the sample is established (as shown in Fig.10). The vertical displacement at the bottom of the model is fixed, and the displacement of the center of the bottom of the model in the vertical and horizontal directions is fixed. According to the test process, the corresponding confining pressure and water pressure are applied. After equilibrium is reached, a deviatoric stress is applied and the temperature is increased to calculate the creep.

A comparison of the axial creep strain curve between the simulation and the test is shown in Fig. 11, and the comparison of the axial creep rate is shown in Fig. 12.

The correlation coefficient between the simulation result of the sample LTHM-1 and the test result is 99.44%; the correlation coefficient of the sample LTHM-2 is 97.67%; the correlation coefficient of the sample LTHM-3 is 98.96%.

It can be seen from the comparison results:

(1) The simulation results can well reflect the stages of decay creep and steady-state creep during the heating process. This is because that at the beginning of creep the creep hardening effect causes the expansion of the creep yield surface and the decrease of overstress and creep rate. As the creep strain increases, the hardening and damage reach equilibrium, the creep yield surface no longer expands, the creep rate stabilises, thereafter entering the steady-state creep stage.

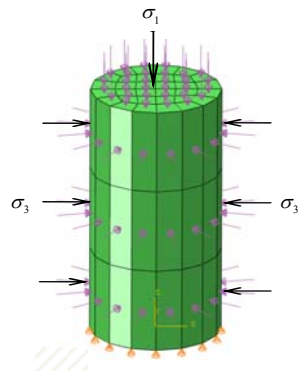

Fig.10 Schematic diagram of the finite element model for test samples

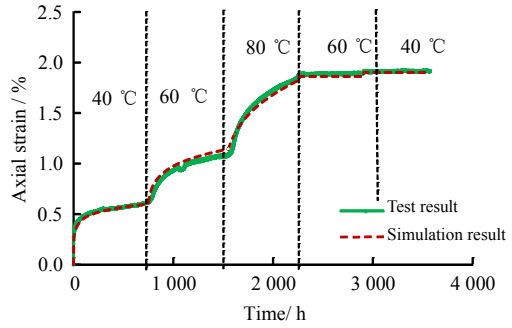

(a) LTHM-1

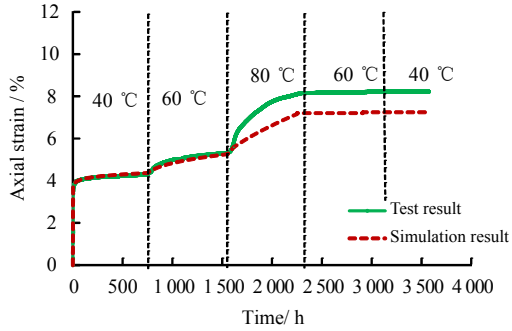

(b) LTHM-2

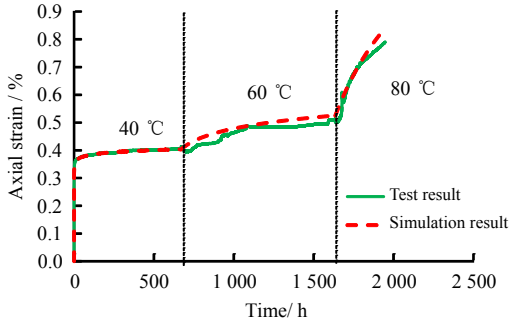

(c) LTHM-3

Fig.11 Comparison of simulated and experimental creep strain curves

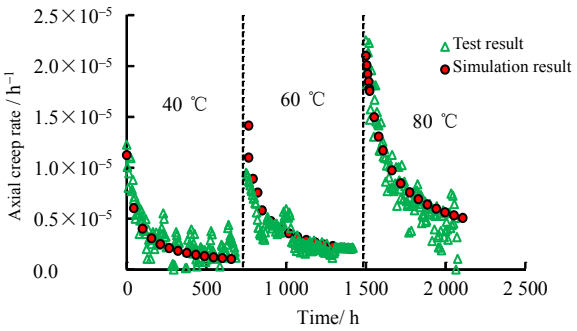

(a) LTHM-1

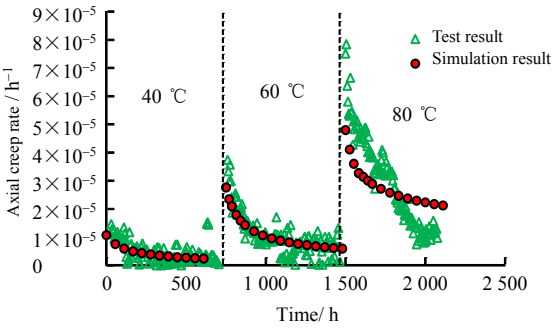

(b) LTHM-2

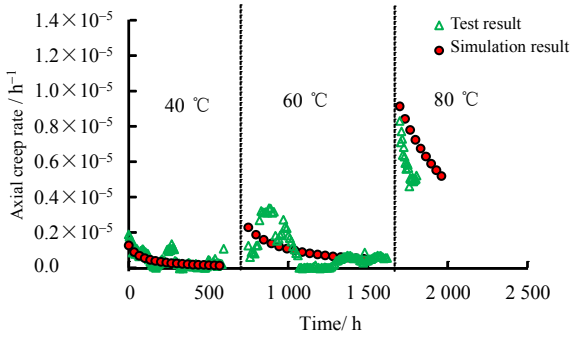

(c) LTHM-3

Fig.12 Comparison of simulated and experimental creep rates

(2) The simulation results also well reflect the effects of temperature, confining pressure and deviatoric stress on creep. As the temperature increases, the confining pressure decreases and the deviatoric stress increases, the simulated creep deformation and creep rate increases significantly. This is because that the creep yield surface takes into account the effects of temperature and stress.

6 Conclusions

In this paper, heating creep tests were conducted on claystone to analyse the influences of temperature, confining pressures and deviatoric stresses on creep characteristics. The following conclusions were drawn:

There exists obvious stages of decay creep and steady-state creep during the heating creep process. Except for a small

amount of cold shrinkage deformation, there is no obvious creep deformation during the cooling process. This is because the increase in temperature will decrease the claystone viscosity and long-term strength, leading to obvious creep phenomenon during heating. Whereas during the cooling process, the viscosity of the sample will gradually recover, making the creep phenomenon less obvious.

An increase in temperature, a decrease in confining pressure, and an increase in deflection stress will significantly increase the creep deformation of the claystone and the creep rate of each creep stage; meanwhile, an increase in temperature will prolong the time of the decay creep stage.

To reflect the experimental research results, this paper introduced thermal damage based on the Perzyna overstress theory, so that the creep yield surface is affected by both stress and temperature. At the same time, the "hardening effect" and "softening effect" in the creep process were considered. Creep hardening and creep damage were introduced to describe these two effects, and a coupled thermo-hydro-mechanical creep model was established. The model was numerically implemented in ABAQUS and its subroutines, and the reliability of the model was verified by the comparison between the simulation results and experimental results.

Reference

[1] LI Y, DIJKSTRA J, KARSTUNEN M. Thermomechanical creep in sensitive clays[J]. Journal of Geotechnical and Geoenvironmental Engineering, 2018, 144(11): 04018085.

[2] KURZ D, SHARMA J, ALFARO M, et al. Semi-empirical elastic-thermoviscoplastic model for clay[J]. Canadian Geotechnical Journal, 2016, 53(10): 1583–1599.

[3] CUI Y J, LE T T, TANG A M, et al. Investigating the time-dependent behaviour of Boom clay under thermo-mechanical loading[J]. Geotechnique, 2009, 59(4): 319–329.

[4] BELMOKHTAR M, DELAGE P, GHABEZLOO S, et al. Thermal volume changes and creep in the Callovo-Oxfordian claystone[J]. Rock Mechanics and Rock Engineering, 2017, 50(9): 2297–2309.

[5] CAMPANELLA R G, MITCHELL J K. Influence of temperature variations on soil behaviour[J]. Journal of the Soil Mechanics and Foundations Division, 1968, 94(SM3): 709–734.

[6] DJÉRAN I, BAZARGAN B, GIRAUD A, et al. Etude expérimentale du comportement thermo-hydro-mécanique de l'argile de Boom[R]. Brussels: ONDRAF, 1994.

[7] BURGHIGNOLI A, DESIDERI A, MILIZIANO S. A laboratory study on the thermomechanical behaviour of clayey soils[J]. Canadian Geotechnical Journal, 2000, 37(4): 764–780.

[8] GAO Feng, XU Xiao-li, YANG Xiao-jun, et al. Research on thermo-visco-elastoplastic model of rock[J]. Chinese Journal of Rock Mechanics and Engineering, 2009, 28(1): 74–80.

[9] LI Jian-guang, WANG Yong-yan. Experimental analysis of temperature effect in creep of soft rock[J]. Journal of China Coal Society, 2012, 37(Suppl.1): 81–85.

[10] SHU Zhi-le, LIU Bao-xian, HUANG Shan, el al. Nonlinear viscoelasto-plastic creep model of soft rock and its parameters identification[J]. Journal of Mining & Safety Engineering, 2017, 34(4): 803–809.

[11] CHEN Wei-zhong, LI Fan-fan, MA Yong-shang, et al. Development of a parallel-linkage triaxial testing machine for THM coupling in soft rock[J]. Rock and Soil Mechanics, 2019, 40(3): 1213–1220.

[12] BERNIER F, VOLCKAERT G, ALONSO E, et al. Suction controlled experiments on Boom clay[J]. Engineering Geology, 1997, 47(4): 325–338.

[13] GONG Zhe. Long-term thermo-hydro-mechanical coupled behaviour of Belgium Boom clay[D]. Wuhan: Institute of Rock and Soil Mechanics, Chinese Academy of Sciences, 2015.

[14] PERZYNA P. Fundamental problems in viscoplasticity[J]. Advances in Applied Mechanics, 1966, 9: 243–377.

[15] PERZYNA P. Thermodynamic theory of viscoplasticity[J]. Advances in applied mechanics, 1971, 11: 313–354.

[16] FRANTIŠEK H. Creep in soft soils[D]. Trondheim: Norwegian University of Science and Technology, 2004.

[17] DAFALIAS Y F. Bounding surface elastoplasticity viscoplasticity for particulate cohesive media[C]// IUTAM Symposium on Deformation and Failure of Granular Materials. Rotterdam: A. A. Balkema, 1982.

[18] ZHOU H, JIA Y, SHAO J F. A unified elastic-plastic and viscoplastic damage model for quasi-brittle rocks[J]. International Journal of Rock Mechanics and Mining Sciences, 2008, 45(8): 1237–1251.

[19] ZHOU H, HU D, ZHANG F, et al. A thermo-plastic/ viscoplastic damage model for geomaterials[J]. Acta Mechanica Solida Sinica, 2011, 24(3): 195–208.

[20] CHEN G J, SILLEN X, VERSTRICHT J, et al. ATLAS III in-situ heating test in Boom clay: field data, observation and interpretation[J]. Computers and Geotechnics, 2011, 38(5): 683–696.

[21] JIA Shan-po. Hydro-mechanical coupled creep damage constitutive model of Boom clay, back analysis of model parameters and its engineering application[D]. Wuhan: Institute of Rock and Soil Mechanics, Chinese Academy of Sciences, 2009.